

## Experiment Report Form

**The double page inside this form is to be filled in by all users or groups of users who have had access to beam time for measurements at the ESRF.**

Once completed, the report should be submitted electronically to the User Office using the **Electronic Report Submission Application:**

*<http://193.49.43.2:8080/smis/servlet/UserUtils?start>*

### ***Reports supporting requests for additional beam time***

Reports can now be submitted independently of new proposals – it is necessary simply to indicate the number of the report(s) supporting a new proposal on the proposal form.

The Review Committees reserve the right to reject new proposals from groups who have not reported on the use of beam time allocated previously.

### ***Reports on experiments relating to long term projects***

Proposers awarded beam time for a long term project are required to submit an interim report at the end of each year, irrespective of the number of shifts of beam time they have used.

### ***Published papers***

All users must give proper credit to ESRF staff members and proper mention to ESRF facilities which were essential for the results described in any ensuing publication. Further, they are obliged to send to the Joint ESRF/ ILL library the complete reference and the abstract of all papers appearing in print, and resulting from the use of the ESRF.

Should you wish to make more general comments on the experiment, please note them on the User Evaluation Form, and send both the Report and the Evaluation Form to the User Office.

### **Deadlines for submission of Experimental Reports**

- 1st March for experiments carried out up until June of the previous year;
- 1st September for experiments carried out up until January of the same year.

### **Instructions for preparing your Report**

- fill in a separate form for each project or series of measurements.
- type your report, in English.
- include the reference number of the proposal to which the report refers.
- make sure that the text, tables and figures fit into the space available.
- if your work is published or is in press, you may prefer to paste in the abstract, and add full reference details. If the abstract is in a language other than English, please include an English translation.



|  |  |                                     |
|--|--|-------------------------------------|
|  | <b>Experiment title: Submicron resolution XRD and Fluorescence tomography applied to wood fiber analysis</b> | <b>Experiment number:</b><br>SC-768 |
| <b>Beamline:</b><br>ID 13  | <b>Date of experiment:</b><br>from: jan -01                      to: nov - 01                                | <b>Date of report:</b><br>25/2 -02  |
| <b>Shifts:</b>   | <b>Local contact(s):</b><br>Christian Riekkel  | <i>Received at ESRF:</i>            |
| <b>Names and affiliations of applicants (* indicates experimentalists):</b><br><b>Anders Rindby</b><br>Chalmers University of Technology, Göteborg, SWEDEN |  |                                     |
| <b>Laszlo Vince</b><br><b>University of Antwerp, Antwerp, Belgium</b>  |  |                                     |

**Report:**

The aim of this project is to apply deconvolution technique in order to achieve sub-micron resolution from the capillary focused micro-beam at ID13. According to calculations, and beam profile simulations, the beam profile should be sharp enough to contain sub-micro components, thus sub-micro structures could, at least in principal, be revealed from deconvolution techniques. However, in order to apply deconvolution technique, the beam profile has to be accurately determined. If the beam profile can be determined, the deconvolution can be applied for any type of 1D or 2D scans. In this project, the deconvolution technique is to be applied in a tomographic mode, to achieve sub-micron structure information, both from XRD as well as XRF spectroscopy.

## Strategy

In order to obtain sub-micro resolution tomography at the present micro-beam set-up at ID13, various technical problems have to be encountered and thus the project has been divided into several phases for trying out different possible solutions for these problems.

The first problem was to accurately determine the beam profile. This can be done by scanning the beam over regular and well-defined structures, which can be recorded from the fluorescent signal. We have used a novel certified reference material developed by IRMM (Institute for Reference Material and Measurements) consisting of perm-alloy (Ni/Fe) strip patterns. This reference material consist of pattern with a size ranging from 100 – 2  $\mu\text{m}$ , fabricated with production schemes from microelectronic circuitry on silicon wafers. The sharpness of the structures should be in the range of 0.1 – 0.2  $\mu\text{m}$ , and the overall precision in strip position should be < 1% according to the test protocol. By scanning the beam over a number of equally spaced strips, with a width of 2  $\mu\text{m}$ , the 1D projection of the beam profile was to be determined from the variation in the Ni fluorescent radiation. The full 2D beam profile was to be determined from a 2D scan over a structure consisting of 4 regularly spaced circles of perm-alloy.

The second problem was the reconstruction of the beam profile from the recorded fluorescent signal. This was in principle done by a “backward” deconvolution technique, where the strip profile were used to deconvolute the actual beam profile. High precision can be achieve for this type of reconstruction if the recorded pattern has a sufficiently high degree of regularity.

The third problem was related to the mechanical precision in the tomographic scanning mode. When doing a tomographic scan, the final resolution will be strongly dependent on the accuracy in the movement induced by the linear and rotational stage during the scan. As we were aiming for sub-micro resolution, the precision in the linear stage should be at least in the order of 0.1  $\mu\text{m}$ , which was not possible for the present set-up. For the rotational stage the stepsize could be made sufficiently small and precise, however, the “wobbling” (non-regular movement of the rotational axis) of the sample, when rotated, would severely deteriorate the resolution in the sinograph, and thus the overall resolution in the reconstructed image. This mechanical imperfection was to be overcome software-wise by using a method for optimal fitting of succesive profiles. Assuming that the sample projection didn't change drastically over an angular increment (about 5 degrees in our test experiment) we would expect that succesive profiles should coincide farly well if the rotational axis is kept fixed. By shifting each profile in the sinograph for maximum fitting to the previous one, the actual “wobbling” could be determined and thus corrected for.

The fourth problem to be encountered was the selfattenuation of the fluorescent radiation in the sample. This is a well known problem in fluorescent tomography and has to be corrected for in order to make proper reconstruction images. In micro-tomography the self-attenuation

is of course small, but for light elements corrections still have to be done. Our approach to this problem was to develop a “in-beam” method for direct determination of the attenuation by rotating the sample 360 degrees rather than the conventional 180 degree scans. By rotating 360 degrees, each projection will be scanned twice, and thus each point will appear twice in a symmetric position in relation to the rotational axis. By comparing corresponding points from profiles shifted 180 degrees, the attenuation can be calculated for each individual point in the sample for any elements recorded. The 360 degrees scan also improve our possibility to establish the “wobbling” movement and thus to correct for it. It also makes it possible to calibrate the angular increment of the scan.

## Experimental achievements so far

Two experimental sessions have been carried out so far within this project. The first experiment was used to scan various part of the IRMM chip, both 1D and 2D scans for beam profile measurements. The primary beam energy was set to about 13 keV and a 2  $\mu\text{m}$  capillary optic unit were used as a post focusing unit. A diode was used to probe the transmitted flux which was used for beam intensity corrections. A solid state driftchamber was used to detect the fluorescent radiation. The detector was placed in the ring-plane in 90 degrees with respect to the primary beam. A piezo stage, with a step size down to 0.1  $\mu\text{m}$ , was used for controlling the sample movement in the beam. A series of 8 parallel strips, with a width of 2  $\mu\text{m}$  were scanned vertically at a 0.1  $\mu\text{m}$  resolution and with 5 seconds of exposure time for each point. Each individual spectra were evaluated with a fitting procedure to allow for a precise determination of peakareas.

At a countrate of about 5000 c/s of Ni radiation the stochastic variation was less than 1% for each point. The time span between each subsequent strip was about 9 minutes. The vertical scan direction would assure that no asymmetry should occur due to self attenuation in the sample.

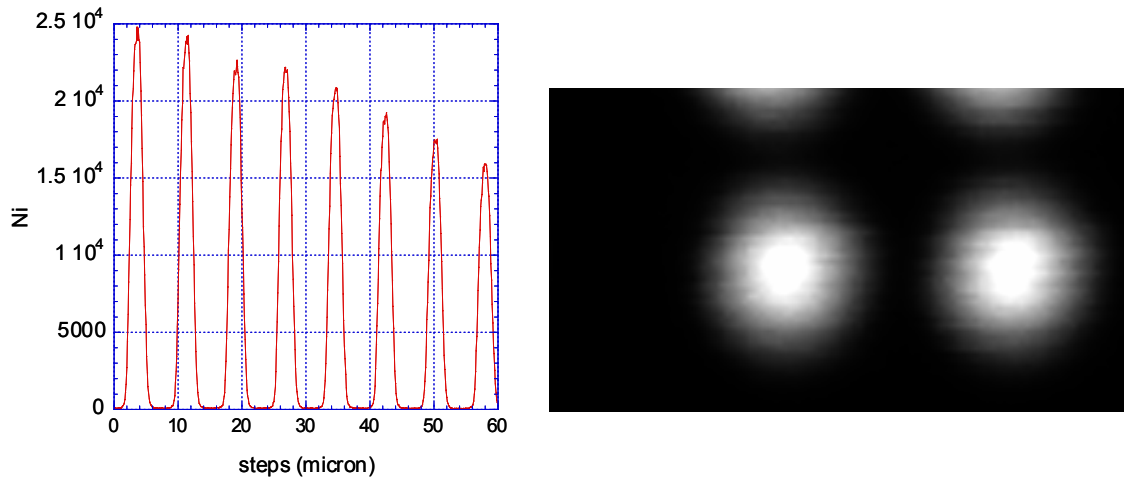
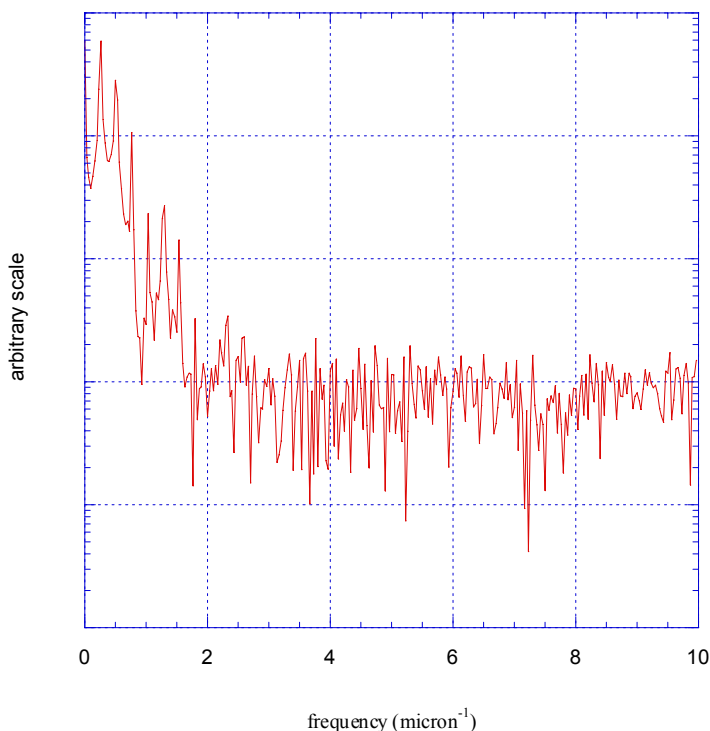


Fig 1 left; 1D scan over regular Ni strips, The strips where 2  $\mu\text{m}$  wide. Right; 2d scan over a block of cylindrical structures, 2  $\mu\text{m}$  in diameter.

The beam profile was reconstructed by deconvoluting the Ni scan with the profile of the actual Ni distribution on the chip. A Fermi function, with a width of 2  $\mu\text{m}$  and a sharpness of 0.1  $\mu\text{m}$ , was used to describe the Ni strips.

2D scans were also performed on 2  $\mu\text{m}$  cylindrical regular structures in order to reveal the 2D beam profile.



In the second experimental session a complete 360 degree tomographic scan were performed on a atomic probe tip. The atomic probe tip consisted manly of WC-Ti(WC) with a binding phase mainly of Co and minor amounts of W, Fe,Cr and Ni. The tip was scanned over a crossection of about 10  $\mu\text{m}$  in diameter. Fluorescence intensity of W, Co, Ni, Fe and scattered radiation were recorded. The scan was performed with a stepsize of 0.3  $\mu\text{m}$  with a angular increment of 5 degrees and 3 seconds of exposure time.

## Results

### *Beam profile measurements*

The 1D projection of the beam profile was determined by deconvolution of the 1D scan over the Ni strips. The Ni peakarea data were carefully evaluated from each spectra recorded (600). Although, the strips were supposed to be regularly spaced and exactly identical, minor deviations were recorded which were beyond the deviation expected from “pure” stochastic

variations. A frequency analysis of the 1D Ni data above shows that the regularity seems to be lost in the white noise at about 0.5  $\mu\text{m}$  level, thus the random variation at this level takes over and no further information can be obtained.

that either, the regularity and/or identity of the strips were not in accordance with the certificate, or the actual beam profile varied slightly with time. The latter explanation is a more probable one as the fine structure in the beam profile, related to the multi-reflexion of the radiation inside the capillary, is very sensitive to the precise beam – source geometry. By deconvoluting each individual strip the beam profile could be determined as a function of time. These profiles shows all the typical characteristics for a capillary beam, but with substantial variation in the fine structures, as can be seen from the figure 3 below.

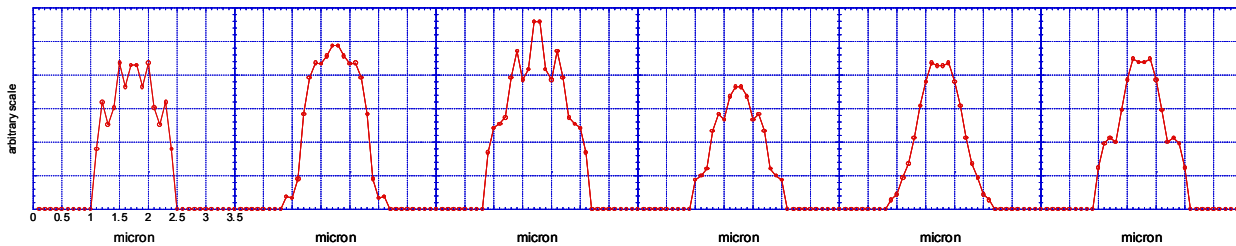


*Fig. 3 Beam profile projection as determined from subsequent Ni strips.*

It is reasonable to believe that the variation in the beam profile, as shown in the figure above, is induced by very small variation in the beam geometry causing amplification and/or suppression of various reflection modes in the beam fine structure. The beam intensity falls only about 5% between each subsequent Ni strip, which still could be sufficient to explain this type of variation. For the 2D scans it should be possible to obtain a full-scale 2D beam profile

from the reconstruction technique, however, here's the scanning time is much larger and thus the time-dependent variations in the beam profile are much more severe. This is clearly demonstrated by the 2D frequency map from the 2D Ni scan in fig. 4.

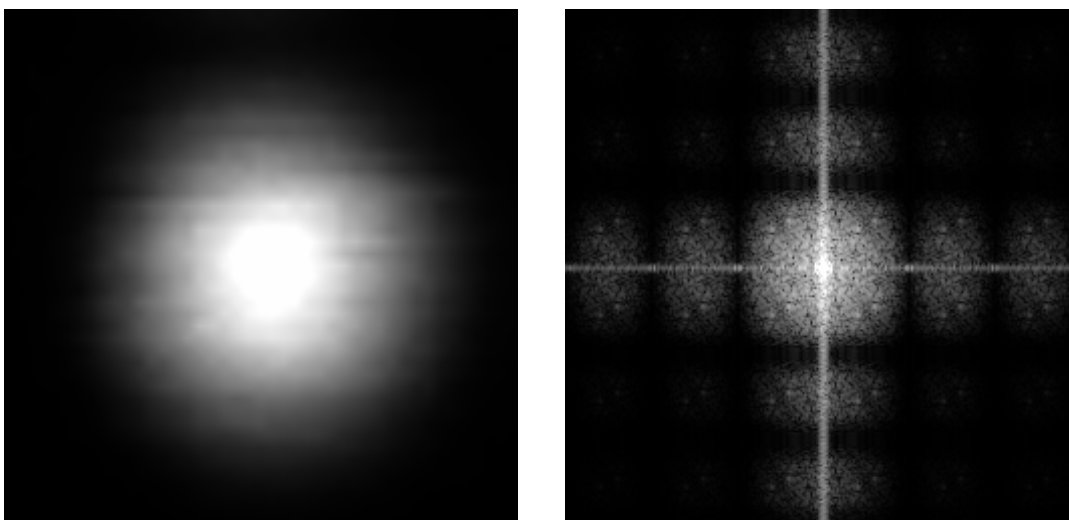


*Fig. 4 left; a 2  $\mu\text{m}$  circular spot of Ni scanned with a stepsize of 0.1  $\mu\text{m}$ , right; the corresponding frequency distribution*

If the beam had been perfectly stable during the scan we would have expected a cylindrical symmetric distribution in phase space, however, due to the time-variation in the beam, the major frequencies will appear in the scanning directions (see above). Instead, the 2D beam profiles were deduced from the 1D scans. By assuming cylindrical symmetry the 2D profiles can be calculated from the 1D projection above. Such a 2D profile would look something like figure 5.

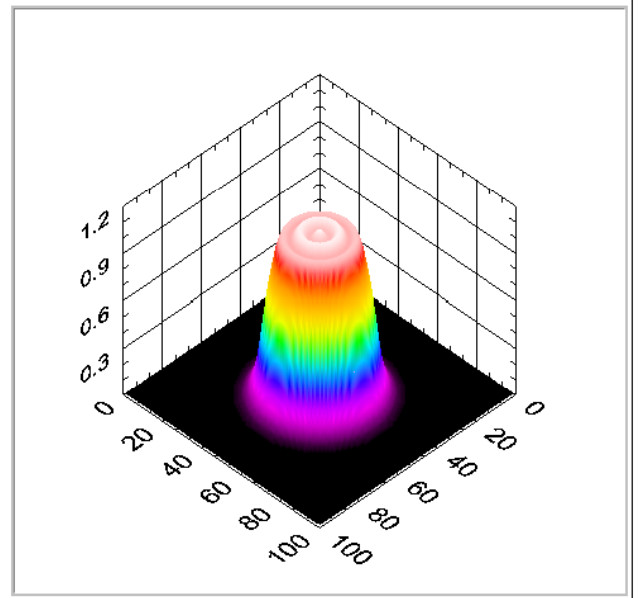


Fig. 5 The complete 2D beam profile reconstruction assuming cylindrical symmetry

#### Tomographic reconstructions

In order to obtain a 1D beam profile projection, useful for deconvolution for the entire tomographic scans, the various beam profiles above were averaged into a single one shown in fig. 6. This profile would at least reveal structures down to the 0.5  $\mu\text{m}$  level. After deconvoluting each individual tomographic scan, each scan was shifted in order to obtain a maximum agreement with the previous one. In this way the wobbling of the rotational stage could be corrected for. The figure below shows the impact of this procedure as on the sinograph as compared with a non-corrected sinograph

From this fitting procedure the wobbling movement could be estimated to be in the order of  $\pm 5 \mu\text{m}$ . By comparing profiles shifted about 180 degrees the angular increment was found to be slightly less than what was specified. A sineodal graph was superimposed on the sinographs to check the fitting procedure and to establish the position of the central axis.

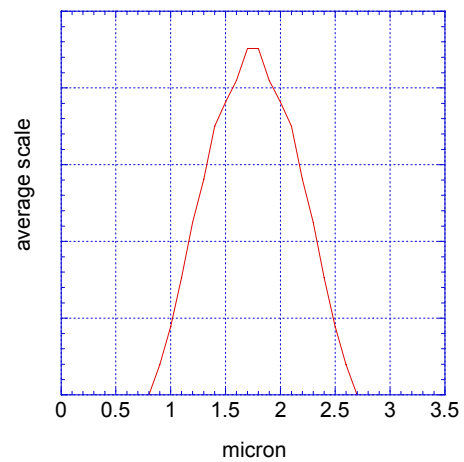


Fig. 6 Average beam profile

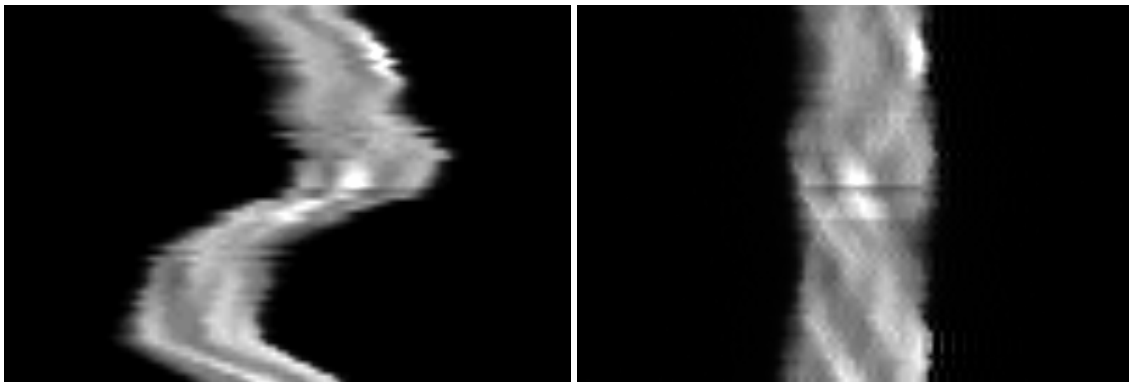


Fig. 7 left; uncorrected sinographs, right; sinographs after fitting procedure

The impact of the deconvolution is demonstrated in figure 8, where sinographs of Ni is shown, both with – and without deconvolution.

The actual tomographs were reconstructed from conventional back-projections, where the “shadow” effects were suppressed by a simple threshold-filtering technique. Some of the tomographs are shown in fig. 9.



*Fig. 8. left Ni sinograph, right; deconvoluted Ni sinograph*

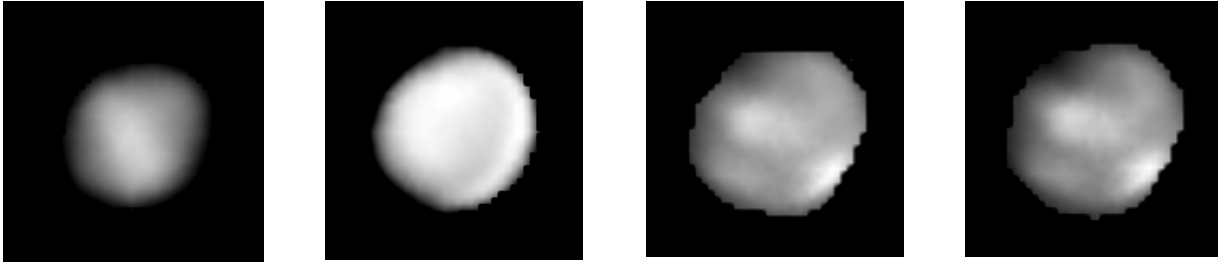


*Fig. 9 full scale tomographic reconstructions from the transmitted radiation (left) and fluorescent radiation (W, Ni and Co)*

We conclude that most of the technical/metrological problem, which were identified in the starting phase, has been tackled in a reasonable way. The results, so far, shows that fluorescent tomography can be performed on a sub-micron scale. However, it seems that beam instability over extended exposure time will limit the resolution to about 0.5  $\mu\text{m}$ .

